

Fidelity and dynamics near Dirac points in two-dimensional systems

Aavishkar A. Patel,¹ Shraddha Sharma,¹ and Amit Dutta¹

¹*Department of Physics, Indian Institute of Technology Kanpur, Kanpur 208016, India*

We study quantum fidelity and dynamics near quantum critical points (QCPs) of the two-dimensional (2-D) Dirac Hamiltonian of graphene (the gapped to gapless transition induced by a mass term) and the 2-D BHZ Hamiltonian of HgTe/CdTe quantum wells (the topological to trivial insulator transition). For the two-dimensional Dirac Hamiltonian, we encounter marginal behaviour of the ground state fidelity near the Dirac point, which is displayed in the absence of a sharp dip in the ground state fidelity (or equivalently the weak logarithmic divergence of the fidelity susceptibility). There is also a logarithmic correction to the proposed scaling of fidelity in the thermodynamic limit. We then study the dynamics of the edge states of the 2-D BHZ Hamiltonian in a ribbon geometry following a sudden quench to the QCP. The effective edge state Hamiltonian is a collection of decoupled two-level systems which get coupled to bulk states following the quench. We notice a pronounced collapse and revival of the Loschmidt echo for low-energy edge states illustrating the oscillation of the state between the two edges. We also observe a similar collapse and revival in the spin Hall current carried by these edge states, leading to a persistence of its time-averaged value.

PACS numbers: 64.70.Tg, 03.65.Pm, 74.40.Kb

The one-dimensional (1-D) and two-dimensional (2-D) Dirac Hamiltonians (DHs) have found a wide range of applications in quantum condensed matter systems in recent years [1–3]. The low-energy physics of graphene [4], and of the bulk states in 2-D topological insulators is described by a 2-D DH [5, 6], and the 1-D edge states existing in a 2-D topological insulator (TI) system are described by an effective 1-D DH [3]. Quantum critical points (QCPs) [7–9] of graphene (the gapless to gapped transition induced by a mass term) as well as the 2-D BHZ Hamiltonian (the topological insulator to trivial insulator transition) are 2-D Dirac points (DPs) with linear dispersions. Experimentally, a gap can be opened in the otherwise gapless linear band structure of graphene through several methods e.g., by the application of an external transverse electric field to the graphene sheet [10]; this is mimicked by adding a mass term to the DH which vanishes at the gapless QCP. The experimental prospect of real-time tuning of parameters controlling these transitions in optical [11, 12] and photonic lattices [13, 14] as well as by exploiting Floquet dynamics [14–17], has made the study of these Hamiltonians from the viewpoint of quantum dynamics timely and necessary.

In this paper, we study the ground state quantum fidelity [18, 19] of a 2-D DH and show the difference in results as compared to the 1-D case. We encounter marginality in the behavior of the ground state fidelity near the DP which shows up in a prominent way both in the scaling of the fidelity susceptibility and the scaling of the fidelity in the thermodynamic limit. The fidelity susceptibility is proportional to the density of defects generated by a sudden quench across a QCP [20, 21]. We then focus on the dynamics of edge states of the BHZ Hamiltonian when the system is suddenly quenched from the TI phase to either the QCP or the trivial insulator (TrI)

phase. The quench couples the two-level subspace of the edge states to a multi-level environment of bulk states. We observe a strong oscillation of the low-energy edge states between the two edges of the system and the persistence of the spin Hall current (SHC) when the system is quenched to the QCP, which we attribute directly to the linear low-energy dispersion at this point (also found in other models describing 2-D TIs).

The ground state quantum fidelity [18] (F), which measures the overlap between many-body ground states at slightly different values of a parameter m of the Hamiltonian, is an important tool for detecting quantum phase transitions [22–25]: one can use the expansion $F = |\langle \psi(m + \delta) | \psi(m) \rangle|^2 = 1 - \delta^2 L^d \chi_F(m) + \dots$, where $\delta (\rightarrow 0)$ is a small change in the parameter m and L is the linear dimension of the d -dimensional system, and $\chi_F(m)$ is defined to be the fidelity susceptibility density at m . The quantum fidelity generally displays a marked drop as m approaches the value m_c at which the Hamiltonian has a QCP. Likewise, χ_F usually diverges in a universal power-law fashion as $|m - m_c|^{2-\nu d}$ where ν is correlation length exponent associated with the QCP [22–24, 26, 27]. We explore the marginal case with $\nu d = 2$, using the example of the 2-D DH with a mass term, while the 1-D case has been found to satisfy the proposed scaling relation with $\nu = d = 1$ [28].

This Hamiltonian can be written in a two-state basis as follows:

$$\mathcal{H}_D = \begin{pmatrix} m & k_x - ik_y \\ k_x + ik_y & -m \end{pmatrix}, \quad (1)$$

where the parameter m is the Dirac mass. This produces two bands with dispersions $E_{\pm} = \pm \sqrt{k_x^2 + k_y^2 + m^2}$, and displays a QCP (DP) at $m = 0$ (with exponent $\nu = 1$) where the gap between the two bands vanishes.

We obtain the fidelity F using the two-level nature of the Hamiltonian (1); for small values of δ , we find

$$F = \exp\left[-\frac{\delta^2 L^2}{16\pi} \left(\frac{m^2}{k_{max}^2 + m^2} - \frac{L^2 m^2}{4\pi^2 + L^2 m^2} + \ln \frac{L^2(k_{max}^2 + m^2)}{L^2 m^2 + 4\pi^2}\right)\right] \quad (2)$$

where k_{max} is an upper cutoff on the \vec{k} modes. Fidelity drops to zero when $k_{max} \rightarrow \infty$ which shows that the high energy modes contribute significantly, which is characteristic of a marginal case (see Fig. 1). The logarithmic scaling of the fidelity susceptibility with m and L also points to the marginality of the situation.

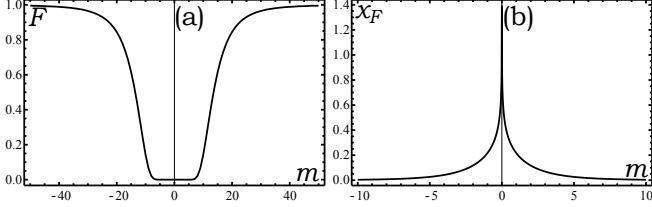


FIG. 1: (a) Fidelity as given by (2), calculated for $\delta = 0.001$ and $L_{x,y} = 10,000$. The fidelity drops to zero at the QCP ($m = 0$) but a sharp dip is absent. (b) The fidelity susceptibility density χ_F has a peak at the QCP.

The most prominent role of marginality manifests in the fidelity studied in the thermodynamic limit ($L \rightarrow \infty$ and small but finite δ), where one cannot use the fidelity susceptibility approach [29]. It has been conjectured that in this limit, $\ln F \sim -\delta^{\nu_d} L^d$ at the QCP; this scaling has been verified for the 1-D DH [28]. In the 2D case, we obtain $\ln F = -L^2 \delta^2 \ln \delta / (8\pi)$. We therefore have a marginal logarithmic correction to the expected δ^2 scaling of the fidelity even in the thermodynamic limit.

We now turn to the 2-D BHZ Hamiltonian describing the low-energy electrons in Hg-Te/Cd-Te quantum well TIs, which displays helical edge state solutions that exist within the bulk bandgap in the TI phase [3, 6]. The bulk states undergo a QPT with the low-energy modes satisfying a 2-D DH with a linear dispersion at the QCP (2-D DP). Additionally, there are chiral edge states with linear dispersion in the TI phase which are described by effective 1-D DH [3]. We study the decoherence of these edge states using the Lochs Schmidt echo (LE) [30] when the 2-D Hamiltonian is quenched from the TI phase to the QCP (or to the TrI phase).

The 4×4 Hamiltonian comprising of two 2×2 blocks (for opposite electron spins) is given by

$$\mathcal{H}_{BHZ} = \begin{pmatrix} H(\vec{k}) & 0 \\ 0 & H^*(-\vec{k}) \end{pmatrix}, \quad (3)$$

where $H(k) = [C - D(k_x^2 + k_y^2)]\mathbf{I}_{2 \times 2} + A[k_x \sigma^x + k_y \sigma^y] +$

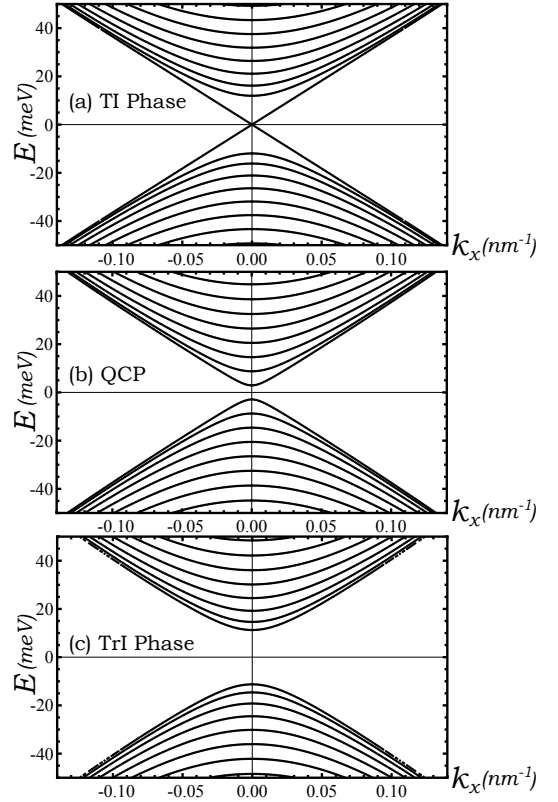


FIG. 2: Spectrum of the BHZ Hamiltonian in a ribbon geometry with ribbon width $L = 200 \text{ nm}$. The parameters used are $A = 364.5 \text{ meV/nm}$, $B = -686 \text{ meV/nm}^2$ and $C = D = 0$. The values of m used are -10 meV (a), 0 (b) and $+10 \text{ meV}$ (c). There is a small gap of $O(A/L)$ in the spectrum near $E = 0$ at $m = 0$ because of the finite width of the ribbon. There also exists an exponentially small gap between the edge state bands in the TI phase. Note the (almost) equal spacing of energy levels for $k_x = 0$ at $m = 0$, characterized by the solutions of a Dirac particle in a 1-D box.

$[m - B(k_x^2 + k_y^2)]\sigma^z$. Here, A, B, C, D and m are determined by the thickness of the quantum well and the material parameters; the parameter m controls the phase of the system and changes sign relative to B when the system crosses from the TI phase (where edge states are present) to the TrI phase (with no edge states) via a DP at $m/B = 0$. This Hamiltonian differs from the previously discussed Hamiltonian (1) by the term $-B(k_x^2 + k_y^2)\sigma^z$, which allows for the existence of edge states which cross the bulk bandgap. Although the results presented here are valid in generic situations, we shall set $D = 0$ for simplicity, which also ensures an electron-hole symmetric spectrum. We consider a ribbon geometry extending from $-L/2$ to $L/2$ in the y direction (with the wavefunction vanishing at the edges) and apply periodic boundary conditions in the x -direction [31–33].

Analyzing Hamiltonian (3), with the given boundary condition, one can show that in the TI phase ($m/B > 0$), there are two types of eigenstates of the Hamiltonian,

i.e., edge states (localized towards the edges and decaying over a length $1/\lambda(k_x, m)$) and bulk states (spreading across the whole ribbon). The spectrum, which is symmetric in $\pm k_x$ and $\pm E$, is displayed in Fig. 2. The edge states in the TI phase exist for $|k_x| < k_0$, k_0 depends on m and L [32].

We perform a sudden quench of the parameter m going from $m/B > 0$ to $m/B \leq 0$ and look at the subsequent evolution of an edge state and its spin current. The edge states, which originally formed a qubit-like two level system with an effective Hamiltonian $H_{edge} \approx Ak_x\sigma_z$ at each k_x [3] now get coupled to several bulk modes and subsequently decohere. Following a sudden quench, the evolution of an edge state is given by

$$|\psi_{edge}(k_x, t)\rangle = \sum_{n=-\infty}^{\infty} \langle\psi_n(k_x)|\psi_{edge}(k_x)\rangle e^{-iE_n t} |\psi_n(k_x)\rangle, \quad (4)$$

where $|\psi_{edge}(k_x)\rangle$ is an edge eigenstate of the Hamiltonian at the initial value of m ($= m_1$) and $|\psi_n(k_x)\rangle$ are the eigenstates of the Hamiltonian at the final value m_2 . The index n runs from $-\infty$ to ∞ excluding $n = 0$ and denotes the -ve and +ve energy bulk modes, respectively. Since all the modes are plane waves along the x direction, different k_x modes do not couple to each other. To study the dynamics of a single edge state and quantify its decay, we calculate the LE $\mathcal{L}(t) = |\langle\psi_{edge}|e^{iH(m_1)t}e^{-iH(m_2)t}|\psi_{edge}\rangle|^2$, which using Eq.(4) can be put in the form

$$\mathcal{L}_{edge}(k_x, t) = \left| \sum_{n=-\infty}^{\infty} |\langle\psi_n(k_x)|\psi_{edge}(k_x)\rangle|^2 e^{-iE_n t} \right|^2. \quad (5)$$

In general, the LE defined above initially drops rapidly with time and turns into a rapidly oscillating noisy function of small amplitude (Fig. 3(a)), indicating that the edge state decoheres significantly. However, there is a striking difference when one looks at the evolution of a low-energy ($k_x \ll k_0$) edge state following a quench to the QCP at $m = 0$; the LE of the edge state shows a pronounced collapse and nearly complete revival for several oscillation cycles (Fig. 3(b)). This is a consequence of the nearly equal spacing of the first few energy levels at low k_x near $m = 0$ (arising due to confinement of the linearly dispersing particles in a ribbon geometry) where the overlap with the edge state is the most significant (see Fig. 2). We then have $E_n \approx \text{sign}(n)[E_g/2 + (|n| - 1)\Delta E]$ for all significant terms in Eq.(4), where $E_g \sim 1/L$ is the bulk bandgap. The summations over $n > 0$ and $n < 0$, then represent Fourier series of a periodic function with period $\tau = 2\pi/\Delta E$ making the LE a periodic function with this period. Since $\mathcal{L}(t = 0) = 1$, the LE shows a near-complete revival at $t = n\tau$. Eventually, after several oscillations, the slight non-uniformity in spacing becomes significant and the revival of the LE weakens.

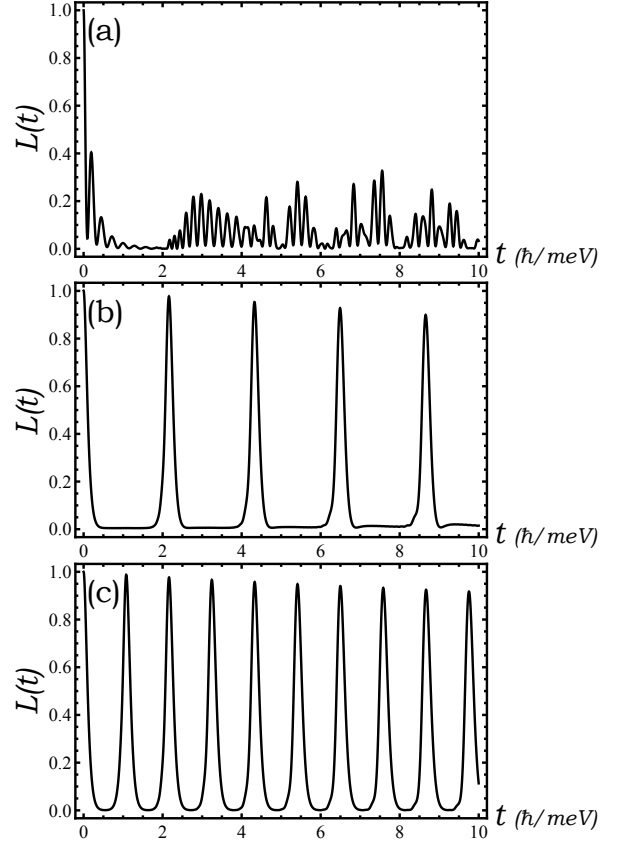


FIG. 3: Looschmidt Echo for various edge states and quenches. The system parameters are $A = 364.5 \text{ meV/nm}$, $B = -686 \text{ meV/nm}^2$, $C = D = 0$ and $L = 400 \text{ nm}$. LE for an edge state with: (a) $k_x = 0.01 \text{ meV/nm}$ and $m = -10 \text{ meV}$ after quenching to $m = +10 \text{ meV}$. There is no significant revival of the edge state. (b) $k_x = 0.001 \text{ meV/nm}$ and $m = -10 \text{ meV}$ after quenching to the QCP at $m = 0$. There is a pronounced collapse to 0 and a nearly full recovery of the LE for several cycles. (c) $k_x = 0$ and $m = -10 \text{ meV}$ after quenching to the QCP. There is a doubling of the frequency of oscillation as compared to the previous case, as this edge state exists on both edges.

Since $\Delta E \sim 1/L$, the period of this revival scales as L . For small quench amplitudes ($|m| \ll A/L$), the edge state does not decay significantly.

Interestingly, we find that the edge state travels from one edge to the other and back, existing on opposite edges at the points of maxima and minima of the LE (Fig. 4(a)). This effect is due to the finite width of the ribbon and will not be seen in an infinite system. Since, for a significantly large system, the edge states at opposite edges do not overlap, the LE drops to zero when the edge state reaches the opposite edge, and revives again when it comes back. For very low values of momentum $k_x \rightarrow 0$, the edge state exists with peaks on both edges of a finite ribbon [31]. Hence, when a peak on a given edge travels to the opposite edge, the peak on the opposite edge also travels simultaneously to the given edge,

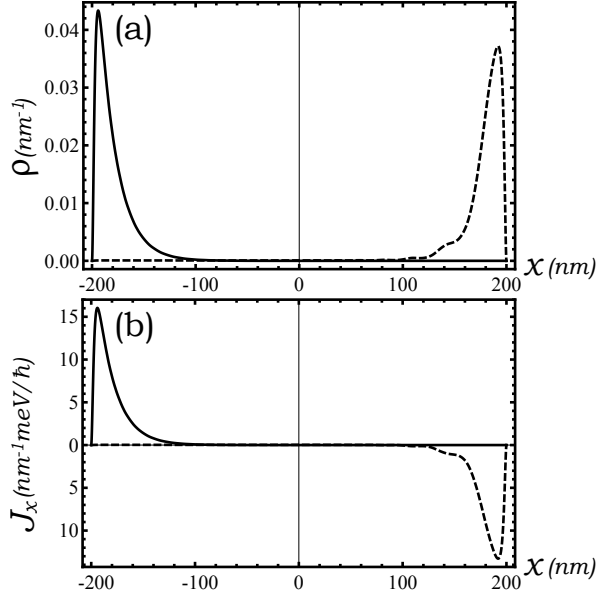


FIG. 4: (a) The probability density $\rho = \psi^\dagger \psi$ of an edge state ($k_x = 0.001 \text{ meV/nm}$) following a sudden quench from $m = -10 \text{ meV}$ to $m = 0$ shown at $t = 0$ (solid) and $t = \tau/2$ (dashed). The edge state travels between the two edges. (b) The probability current density of the state in the x direction (J_x) at $t = 0$ (solid) and $t = \tau/2$ (dashed). The same state carries currents of opposite direction on opposite edges. The system parameters are the same as Fig. (3).

resulting in a maximum of the LE at $(2n+1)\tau/2$ instead of a minimum, and hence a doubling of the frequency of oscillation of the LE. The LE is now minimum at times when the state is concentrated near the middle of the ribbon (Fig. 3(c)).

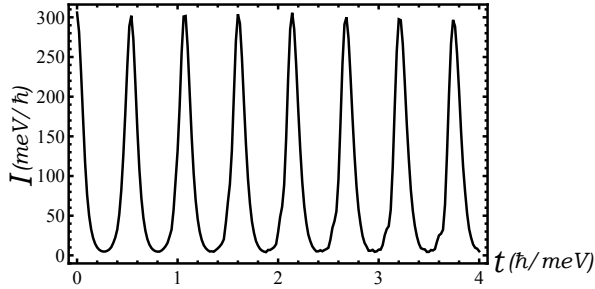


FIG. 5: The net probability current carried by the pair of edge states with $E = 3.65 \text{ meV}$ (near the $-L/2$ edge over a length $1/\lambda \approx 37 \text{ nm}$) following a quench from $m = -10 \text{ meV}$ to $m = 0$. The current collapses and revives like the LE, and is always greater than zero, leading to a persistence of its time-averaged value. The system parameters are $A = 364.5 \text{ meV/nm}$, $B = -686 \text{ meV/nm}^2$, $C = D = 0$ and $L = 200 \text{ nm}$.

The probability current carried near the edge in the x direction by the edge states over their decay length $1/\lambda$ is proportional to the net SHC carried by the state and its time-reversed conjugate in the opposite spin sector.

It can be calculated using the continuity equation for the probability current density \vec{J} in conjunction with the Schrodinger time evolution equation

$$\begin{aligned} \frac{\partial}{\partial t} [\psi^\dagger(x, y, t)\psi(x, y, t)] + \nabla \cdot \vec{J} &= 0, \\ i\frac{\partial}{\partial t}\psi(x, y, t) &= H\psi(x, y, t), \end{aligned} \quad (6)$$

where $\psi(x, y, t)$ is a two component wavefunction of the form $\psi(x, y, t) = (\phi_1(y, t), \phi_2(y, t))e^{ik_x x}$; we obtain

$$\begin{aligned} J_x(y, t) &= 2A \text{Re} [\phi_1(y, t)\phi_2^*(y, t)] + \\ &2Bk_x [|\phi_2(y, t)|^2 - |\phi_1(y, t)|^2]. \end{aligned} \quad (7)$$

For $k_x \rightarrow 0$, the first Dirac-like term dominates the second Schrodinger-like term, implying that all low-energy edge states carry virtually the same current. The profile of J_x is shown at the instants of time when the edge state exists on opposite edges in Fig. 4(b). The sign of the current reverses when the state moves to the opposite edge.

The evolution of the SHC carried by edge states of a given energy near a given edge (say, $-L/2$) can be obtained by integrating J_x from $-L/2$ to $-L/2 + 1/\lambda$. Since there are two oppositely propagating edge states at a given energy which exist on opposite edges of the system, we must add the currents carried by both of them. The time evolution of such a current following a sudden quench to the QCP is shown in Fig. 5. This current also displays a pronounced collapse and revival for several cycles when the LE does so. The time-averaged value of the current is non-zero and is a significant fraction of the original value of the current. Thus, there is a persistence of the SHC carried by low-energy edge states following a sudden quench to the QCP.

To summarize, the quantum fidelity shows a markedly different behavior for the 2-D DH in comparison to the 1-D case. We observe interesting decoherence dynamics of the low-energy edge states of a TI Hamiltonian when quenched to the QCP displayed in the temporal evolution of their LE. Given the recent prospects of tuning of control parameters of the related Hamiltonians, we believe that this study is of experimental relevance.

We acknowledge Apoorva Patel and Diptiman Sen for helpful discussions. AAP acknowledges the KVPY fellowship and AD and SS acknowledge CSIR, New Delhi, for financial support.

-
- [1] A. H. Castro Neto, F. Guinea, N. M. R. Peres, K. S. Novoselov and A. K. Geim, Rev. Mod. Phys. **81**, 109 (2009).
 - [2] M.H. Hasan, C.L. Kane, Rev. Mod. Phys. **82**, 3054 (2010).

- [3] Xiao-Liang Qi, Shou-Cheng Zhang, *Rev. Mod. Phys.* **83**, 1057 (2011).
- [4] K. Novoselov, A. Geim, S. Morozov, D. Jiang, M. Grigorieva, S. Dubonos, and A. Firsov, *Nature* **438**, 197 (2005).
- [5] C. L. Kane and E. J. Mele, *Phys. Rev. Lett.* **95**, 226801 (2005).
- [6] B. Bernevig, T. Hughes, and S. Zhang, *Science* **314**, 1757 (2006).
- [7] S. Sachdev, *Quantum Phase Transitions* (Cambridge University Press, Cambridge, England, 1999).
- [8] B. K. Chakrabarti, A. Dutta, and P. Sen, *Quantum Ising Phases and transitions in transverse Ising Models*, m41 (Springer, Heidelberg, 1996).
- [9] S. L. Sondhi, S. M. Girvin, J. P. Carini, and D. Shahar, *Rev. Mod. Phys.* **69**, 315 (1997).
- [10] R. Quhe, J. Zheng, G. Lou, Q. Liu, R. Qin, J. Zhou, D. Yu, S. Nagase, W-N. Mei, Z. Gao, and J. Lu, *NPG Asia Materials* **4**, e6 (2012).
- [11] K. L. Lee, B. Gremaud, R. Han, B-G Englert, and C. Miniatura, *Phys. Rev. A* **80**, 043411 (2009).
- [12] T. D. Stanescu, V. Galitski, J. Y. Vaishnav, C. W. Clark, and S. Das Sarma, *Phys. Rev. A* **79**, 053639 (2009).
- [13] T. Ochiai and M. Onoda, *Phys. Rev. B* **80**, 155103 (2009).
- [14] M. C. Rechtsman, J. M. Zeuner, Y. Plotnik, Y. Lumer, S. Nolte, M. Segev, A. Szameit, arXiv:1212.3146 (2012).
- [15] T. Oka and H. Aoki, *Phys. Rev. B* **79**, 081406 (2009).
- [16] H. L. Calvo, H. M. Pastawski, S. Roche and L. E. F. Foa Torres, *Appl. Phys. Lett.* **98**, 232103 (2011).
- [17] N. H. Lindner, G. Refael and V. Galitski, *Nat. Phys.* **7**, 1926 (2011).
- [18] P. Zanardi and N. Paunkovic, *Phys. Rev. E* **74**, 031123 (2006).
- [19] H-Q. Zhou and J. P. Barjaktarevic, *J. Phys. A: Math. Theor.* **41** 412001 (2008).
- [20] C. De Grandi, V. Gritsev and A. Polkovnikov, *Phys. Rev. B* **81**, 012303 (2010).
- [21] A. A. Patel and A. Dutta, *Phys. Rev. B* **86** 174306 (2012).
- [22] L. Campos Venuti and P. Zanardi, *Phys. Rev. Lett.* **99**, 095701 (2007), P. Zanardi, P. Giorda, and M. Cozzini, *Phys. Rev. Lett.* **99**, 100603 (2007).
- [23] Shin-Jian Gu, *Int. J. Mod. Phys. B* **24**, 4371(2010).
- [24] A. Dutta, U. Divakaran, D. Sen, B. K. Chakrabarti, T. F. Rosenbaum and G. Aeppli, arXiv:1012.0653 (2010).
- [25] H-Q. Zhou, R. Orus and Guifre Vidal, *Phys. Rev. Lett.* **100**, 080601 (2008).
- [26] V. Gritsev and A. Polkovnikov, arXiv:0910.3692 (2009), published in *Understanding Quantum Phase Transitions*, edited by L. D. Carr (Taylor and Francis, Boca Raton, 2010).
- [27] D. Schwandt, F. Alet, and S. Capponi, *Phys. Rev. Lett.* **103**, 170501 (2009); A. F. Albuquerque, Fabien Alet, Clement Sire, and Sylvain Capponi, *Phys. Rev. B* **81**, 064418 (2010).
- [28] V. Mukherjee, A. Dutta and D. Sen, *Phys. Rev. B* **85**, 024301 (2012).
- [29] M. M. Rams and B. Damski, *Phys. Rev. Lett.* **106**, 055701 (2011); M. M. Rams and B. Damski, *Phys. Rev. A* **84** 032324 (2011).
- [30] H. T. Quan, Z. Song, X. F. Liu, P. Zanardi, and C. P. Sun, *Phys. Rev. Lett.* **96**, 140604 (2006).
- [31] B. Zhou, H. Z. Lu, R. L. Chu, S. Q. Shen, and Q. Niu, *Phys. Rev. Lett.* **101**, 246807 (2008).
- [32] M. Konig, H. Buhmann, L. W. Molenkamp, T. Hughes, C-X. Liu, X-L. Qi and S-C. Zhang, *J. Phys. Soc. Jpn.* **77** 031007 (2008).
- [33] M. Wada, S. Murakami, F. Freimuth and G. Bihlmayer, *Phys. Rev. B* **83**, 121310(R) (2011).